Macromolecules **2005,** *38,* 8170−8176

Kinetics and Mechanism of Cyclic Esters Polymerization Initiated with Tin(II) Octoate. Polymerization of ϵ-Caprolactone and L,L-Lactide Co-initiated with Primary Amines

Adam Kowalski, Jan Libiszowski, Tadeusz Biela, Marek Cypryk, Andrzej Duda,* and Stanislaw Penczek

Department of Polymer Chemistry, Center of Molecular and Macromolecular Studies, Polish Academy of Sciences, 90-363 Lodz, Sienkiewicza 112, Poland

Received April 11, 2005; Revised Manuscript Received July 12, 2005

ABSTRACT: Following our previous papers on the mechanism of ϵ-caprolactone (CL) and L,L-lactide (LA) polymerization initiated by tin(II) octoate [(tin(II) bis(2-ethylhexanoate), ($Sn(Oct)_2$)] in the presence of the hydroxyl-group-containing compounds [H_2O, alcohols or hydroxy-carboxylic acids (ROH)] the present work shows that the CL or LA/$Sn(Oct)_2$/primary amine (RNH_2) system, in principle, does not differ mechanistically from the CL or LA/$Sn(Oct)_2$/ROH system. ^{1}H NMR, matrix-assisted laser desorption and ionization time-of-flight (MALDI-TOF) mass spectrometric and kinetic studies reveal that, in the first step of polymerization initiated with the $Sn(Oct)_2/RNH_2$ mixtures, formation of the α-amido-ω-alcohol (RNH-m-H (R′OH)) (in which m denotes the repeating unit derived from CL or LA) proceeds. Then, the further steps of polymerization follow with R′OH as co-initiator. Thus, eventually, the $Sn(Oct)_2/RNH_2$-initiated polymerization proceeds by the monomer insertion into the ...-Sn−OR″ bond, reversibly formed in the reaction: ...-SnOct + R″OH ⇌ ...-Sn−OR″ + OctH, in which R″OH is either the low-molar-mass co-initiator (R′OH) or a macromolecule fitted with the hydroxyl end group (RNH-$(m)_n$-H); OctH stands for 2-ethylhexanoic (octanoic) acid. These interconversions take place throughout the entire polymerization process. The $Sn(Oct)_2$/amino dendrimer (e.g., commercially available DAB−Am-8 and DAB−Am-32, polyamines, fitted with 8 and 32 primary amino groups) system acts in a similar way. Molar masses of the resulting star-shaped polymer, in which polyester chains bear the hydroxyl end groups, are controlled by the monomer and dendrimer concentrations ratio in the feed.

Introduction

Tin octoate [tin(II) bis(2-ethyl hexanoate), $Sn(Oct)_2$] is probably the most often used initiator in the polymerization of cyclic esters. However, it was also the least understood, and several initiation pathways with $Sn(Oct)_2$ were proposed.[1−7] In a majority of those mechanisms, co-initiation with a hydroxyl-group-containing compound [e.g., H_2O, alcohol, or hydroxy-carboxylic acid (denoted further as ROH)] has been assumed. We showed, on the basis of both a direct observation of Sn atoms in the polyester chains and of kinetic studies, that at least one of the active species, directly observed by matrix-assisted laser desorption and ionization time-of-flight (MALDI-TOF) mass spectrometry, is OctSnOR, reversibly formed as it is schematically shown in eq 1a. The results of kinetics studies of cyclic esters polymerization initiated with "pure" $Sn(Oct)_2$, $Sn(OR)_2$, and $Sn(Oct)_2$/ROH and $Sn(OR)_2$/octanoic acid mixtures also revealed that the actual initiator is the tin(II) alkoxide, formed in the exchange reactions between carboxylate and alkoxide ligands in $Sn(Oct)_2$ and ROH, respectively:[8−13]

$$\mathrm{Sn(Oct)_2} + \mathrm{ROH} \rightleftharpoons \mathrm{RO\text{-}Sn\text{-}Oct} + \mathrm{OctH} \tag{1a}$$

$$\mathrm{RO\text{-}Sn\text{-}Oct} + \mathrm{ROH} \rightleftharpoons \mathrm{RO\text{-}Sn\text{-}OR} + \mathrm{OctH} \tag{1b}$$

(where: Oct = $C_4H_9CH(C_2H_5)C(O)O$). Then, further steps of polymerization proceed with tin(II) mono- or dialkoxides as with other covalent metal alkoxides.

Independently, it has been reported that, in the $Sn(Oct)_2$-initiated polymerization of cyclic esters, primary amines (RNH_2) can also serve as co-initiators.[11,14] More recently, polymerization of ϵ-caprolactone (CL) initiated by natural amino acids at elevated temperatures has been reported.[15] These observations open new possibilities, e.g., in the synthesis of polypeptide-poly(aliphatic ester) block copolymers or star-shaped copolymers based on polyamino dendrimers. Therefore, we have studied the $Sn(Oct)_2/RNH_2$ system in more detail.

The present paper aims at reporting the kinetics and mechanism of CL and L,L-lactide (LA) polymerization initiated with $Sn(Oct)_2/BuNH_2$ or $Sn(Oct)_2$/polyamino dendrimer mixtures and the synthesis of star-shaped poly(CL) and poly(LA) based on commercially available dendrimers DAB−Am-8 and DAB−Am-32, bearing 8 and 32 terminal NH_2 groups, respectively.

Experimental Section

Materials. ϵ-Caprolactone (CL), (99%, Aldrich) after fractionated distillation from CaH_2 under reduced pressure (2 mbar, 98 °C), was kept in vacuo over molecular sieves (4 Å). Then it was finally purified by two consecutive vacuum distillations to ampules with fresh Na mirrors. L,L-Lactide (LA) (99%, Boehringer Ingelheim, Germany) and D,D-lactide (LA) (99%, Purac, Netherlands), crystallized consecutively from dry 2-propanol and toluene, were purified just before use by sublimation in vacuo (10^{-3} mbar, 85 °C). Purified monomers were distributed into ampules equipped with breakseals and stored at −12 °C). Tin(II) 2-ethylhexanoate ($Sn(Oct)_2$) commercial product (Aldrich) contains, according to our determinations, about 20 mol % of "acidic" impurities. Two consecutive high-vacuum distillations resulted in $Sn(Oct)_2$, showing in ^{1}H NMR spectra 1.8 mol % of the "acidic" protons (fraction distilling at 140 °C/3 × 10^{-3} mbar), which may correspond to

---

* Author to whom correspondence should be addressed. E-mail: anduda@bilbo.cbmm.lodz.pl. Telephone: +48-42-681 9815. Fax: +48-42-684 7126.

10.1021/ma050752j CCC: \$30.25

0.9 mol % of H_2O content. Thus, purified $Sn(Oct)_2$, kept all of the time in vacuo, was finally distributed directly into the thin-walled glass vials and sealed off. Butylamine ($BuNH_2$) (99%, Aldrich) and *N*-methylacetamide (NMA) (99+%, Aldrich) were kept over CaH_2. Butyl alcohol (BuOH) (99+%, Aldrich) was dried with Na metal. All these reagents were then distributed by distillation in vacuo into the thin-walled glass vials. Tetrahydrofuran (THF) (98%, POCh, Gliwice, Poland), kept several days over KOH pellets, was decanted and distilled from Na metal chips over a Na/K metals liquid alloy, from which it was distilled in vacuo directly into the reaction vessel. $CDCl_3$ (99%, Dr Glaser AG, Basel, Switzerland) was dried by distillation from CaH_2 before use. Dendrimeric polyamines DAB−Am-8 and DAB−Am-32 (from Aldrich, DSM products) were dried 24 h under vacuum (10^{-3} mbar/50 °C) before use.

Determination of Monomer Conversions. Kinetics of CL polymerization was followed in all-glass dilatometers sealed under high vacuum. That of LA was determined using polarimetric measurements, performed with a Perkin-Elmer 241 MC polarimeter at room temperature. The optical rotations (*or*) of the living polymerization mixtures were measured at 578 nm. The instantaneous monomer concentrations were determined, assuming additivity of the optical rotations for LA (or_m) and PLA (or_p), i.e., $[LA] = [LA]_0\ (or - or_p)/(or_m - or_p)$.

Concentrations of CL and LA were occasionally checked by size exclusion chromatography (SEC) measurements, confirming readings obtained by dilatometry and polarimetry, respectively. SEC traces were recorded using a LKB 2150 HPLC pump, two sets of TSK gel columns (G 2000 H_{XL} and 6000 H_{XL} or G 3000 H_{HR} and G 6000 H_{HR} with pore sizes 2.5×10^2 and 10^6 or 1.5×10^3 and 10^6 Å, respectively) at 20 °C. Wyatt Optilab 903 interferometric refractometer ($\lambda = 690$ nm) and multiangle laser light scattering (MALLS) Dawn F laser photometer, equipped with an He−Ne laser emitting at 632.8 nm (both Wyatt Technology Corp., Santa Barbara, CA), were applied as detectors in series. Methylene chloride was used as an eluent at a flow rate of 0.8 mL min^{-1}.

Determination of Molar Masses (M_n) and Molar-Mass Distributions (M_w/M_n). The actual number-average molar masses of poly(CL) and poly(LA) were determined using size exclusion chromatography (SEC), osmometry, and ^1H NMR spectroscopy. The M_w/M_n ratios were determined from the SEC traces. M_n values higher than 10^4 were directly determined with a MALLS Dawn F laser photometer and using the ASTRA v 4.70 program (Wyatt Technology Corp., Santa Barbara, CA). The refractive index increments [$dn/dc = 0.048$ and 0.026 for poly(CL) and poly(LA), respectively] were determined from refractive index concentration dependencies obtained with a Wyatt Optilab 903 interferometric refractometer. For measurements of M_n exceeding 10^5, a set of TSK gel G 3000 H_{HR} and G 6000 H_{HR} columns was used. In osmometric measurements, Knauer vapor pressure or high-speed membrane osmometers for $M_n \leq 3.5 \times 10^4$ or $\geq 3.5 \times 10^4$, respectively, were used by employing dry methylene chloride as solvent.

NMR Measurements. ^1H NMR spectra were recorded in $CDCl_3$ on Bruker AC200 (200 MHz) or Bruker DRX 500 (500 MHz) spectrometers.

MALDI-TOF Measurements. Mass spectrometric measurements were performed using a Voyager-Elite (PerSeptive Biosystems, Framingham, MA) time-of-flight instrument equipped with a pulsed N_2 laser (337 nm, 4 ns pulse width) and time-delayed extraction ion source. An accelerating voltage of 20 kV was used. Mass spectra were obtained in the reflector and/or linear mode. The matrix, 2,5-dihydroxybenzoic acid, was dissolved in THF or methylene chloride at a concentration equal to 10 mg mL^{-1}, and the solution was mixed with the polymerizing mixture (monomer concentration in the feed: 1.0 mol L^{-1}) in a 25:1 v/v ratio. NaI was added as a cationizing agent. The mixture was dried on a stainless steel plate covered by the gold metal target.

Polymerization Procedures. A general procedure is described using the example given below. $Sn(Oct)_2$ (1 mL of 0.75 mol L^{-1} solution in dry THF) and LA (2.16 g, 15 mmol) were transferred under vacuum into breakseals and sealed after freezing in liquid nitrogen. $BuNH_2$ (0.132 g, 1.8 mmol) was distilled into a thin-walled glass vial and then sealed after freezing in liquid nitrogen. Breakseals containing $Sn(Oct)_2$/THF solution and LA monomer, a tube with an immersed $BuNH_2$ vial, polarimetric cell, and glass ampules were sealed to the reacting (≈ 30 mL) glass vessel. THF (12.2 mL) was distilled into the resulting reactor, which was then sealed off. The breakseals and the vial were broken, and then all components were dissolved at room temperature. The resulting solution was transferred into the polarimetric cell and the glass ampules. The cell and ampules containing reacting mixture were then sealed off and placed into a thermostat (80 °C). The *or* of the reacting mixture was measured at room temperature in approximately 10 min intervals until it reached a constant value. Then the reacting mixture was injected into a SEC apparatus. Analysis of a SEC trace of the crude reacting mixture gave $M_n = 1.7 \times 10^3$, $M_w/M_n = 1.35$ and 96% of LA conversion (in these conditions $[LA]_{eq} = 0.055$ mol L^{-1}. The resulting poly(LA) (BuNH−PLA-H) was precipitated into cold heptane, separated by filtration, and washed several times with heptane, up to a disappearance of the unreacted $Sn(O(O)CCH(C_2H_5)C_4H_9)_2$ protons NMR absorption (e.g., the −CH− multiplet at $\delta = 2.1$ ppm). Mass of the vacuum-dried product and its M_n measured osmometrically were equal to 2.05 g (90% yield) and 1.1×10^3, respectively. ^1H NMR spectrum analysis ($CDCl_3$, 20 °C) gave the following results (chemical shifts (δ, in ppm),[11] multiplicities of signals, and their relative intensities are given in brackets):

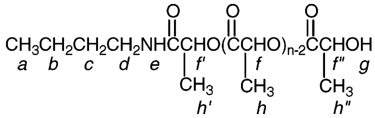
$$\underset{a}{CH_3}\underset{b}{CH_2}\underset{c}{CH_2}\underset{d}{CH_2}\underset{e}{NH}\overset{O}{\overset{\|}{C}}\underset{\underset{h'}{CH_3}}{\underset{|\,f'}{C}}HO(\overset{O}{\overset{\|}{C}}\underset{\underset{h}{CH_3}}{\underset{|\,f}{C}}HO)_{n-2}\overset{O}{\overset{\|}{C}}\underset{\underset{h''}{CH_3}}{\underset{|\,f''}{C}}H\underset{g}{OH}$$

a (0.9, t, 3.00), *b*+*c* (1.3, m, 3.44), *d* (3.25, q, 2.19), *e* (6.15, t, 1.01), *f*+*f′* (5.15, q, 13.10), *f″* (4.31, q, 1.10), and *g* (2.8, broad signal, 0.95). M_n calculated on the basis of NMR data is equal to 1.065×10^3. Both M_n(osm) and M_n(NMR) are close to 1208, a value predicted from the feed composition ($M_n(calcd) = M_{LA}([LA]_0 - [LA]_{eq})/[BuNH_2]_0 + M_{BuNH2}$, where $M_{LA} = 144.13$ and $M_{BuNH2} = 73.14$).

Polymerizations of CL were carried out in a similar way. The only difference was that the polarimetric cells were substituted by dilatometers equipped with capilary tubes. Dilatometers were put in the precisely thermostated (± 0.05 deg) water bath in order to perform accurate measurements of the reacting mixture volume changes during polymerization (actually measurements of the meniscus level in the capilary tube). For the isolated poly(CL) (BuNH−PCL-H), the following ^1H NMR chemical shifts assignments agree with those already reported in ref 16:

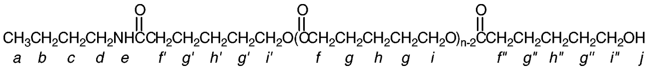
$$\underset{a}{CH_3}\underset{b}{CH_2}\underset{c}{CH_2}\underset{d}{CH_2}\underset{e}{NH}\overset{O}{\overset{\|}{C}}\underset{f'}{CH_2}\underset{g'}{CH_2}\underset{h'}{CH_2}\underset{g'}{CH_2}\underset{i'}{CH_2}O(\overset{O}{\overset{\|}{C}}\underset{f}{CH_2}\underset{g}{CH_2}\underset{h}{CH_2}\underset{g}{CH_2}\underset{i}{CH_2}O)_{n-2}\overset{O}{\overset{\|}{C}}\underset{f''}{CH_2}\underset{g''}{CH_2}\underset{h''}{CH_2}\underset{g''}{CH_2}\underset{i''}{CH_2}\underset{j}{OH}$$

a (0.9, t, 3.00), *b*+*c* (1.3, m, not measured), *d* (3.25, q, 2.08), *e* (7.0, m, 1.02), *f′* (2.19, t, 1.88), *f*+*f″* (2.34, t, 32.3), *g′*+*g*+*g″* (1.65, m, 24.51), *h′*+*h*+*h″* (1.41, m, 11.94), *i′*+*i* (4.08, t, 10.76), *i″* (3.65, t, 2,16), and *j* (3.90, m, broad signal, 0.96). In the given example, 15 mmol of CL and 2.25 mmol $BuNH_2$ in the feed was used. Thus, $M_n(calcd) = M_{CL}\ [CL]_0/[BuNH_2]_0 + M_{BuNH2} = 834$ (where $M_{CL} = 114.14$ and $M_{BuNH2} = 73.14$). Osmometric measurements and analysis of the ^1H NMR spectra gave $M_n(osm) = 920$ and $M_n(NMR) = 1013$, respectively.

Theoretical Methods. Density functional (DFT) molecular orbital calculations were carried out on a Opteron-based PC cluster using the Gaussian 03 program.[17] Geometry optimizations were performed using standard techniques at the B3LYP level of theory.[18] The pseudopotential basis set LANL2DZ was used as defined in Gaussian.[19,20] All ground states were verified by vibrational frequency analysis. Enthalpy corrections were calculated for 298 K from frequency calculations (scaling factor of 0.98 was applied).

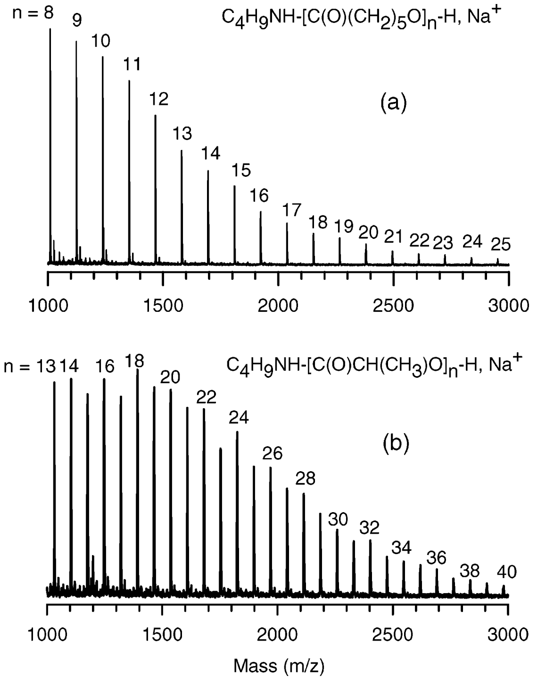

Figure 1. Matrix-assisted laser desorption and ionization time-of-flight (MALDI-TOF) mass spectra of the ϵ-caprolactone (CL)/tin(II) octoate [(tin(II) bis(2-ethylhexanoate), ($Sn(Oct)_2$)]/butylamine ($BuNH_2$) (a) and (L,L-lactide) LA/$Sn(Oct)_2$/$BuNH_2$ (b) reacting mixtures (linear mode, sample doped with NaI). Conditions of polymerization: $[CL]_0 = 1.0$ mol L^{-1}, $[Sn(Oct)_2]_0 = 0.01$ mol L^{-1}, $[BuNH_2]_0 = 0.15$ mol L^{-1} (a); $[LA]_0 = 1.0$ mol L^{-1}, $[Sn(Oct)_2]_0 = 0.05$ mol L^{-1}, $[BuNH_2]_0 = 0.12$ mol L^{-1}; tetrahydrofuran (THF), 80 °C.

Results and Discussion

CL and LA Polymerizations Initiated with the $Sn(Oct)_2$/$BuNH_2$ System. MALDI-TOF mass spectra of the reacting mixtures show almost exclusively the presence of signals corresponding to C_4H_9NH-$[C(O)(CH_2)_5O]_n$-H and C_4H_9NH-$[C(O)CH(CH_3)O]_n$-H chains (Figure 1).

The ^1H NMR data are consistent with the polyester chain microstructures determined by means of mass spectrometry. Moreover, molar masses of the polyesters are controlled by monomers and $BuNH_2$ co-initiator concentrations in the feed, every molecule of $BuNH_2$ starts growth of exactly one polyester chain being transformed into the amido tail end group (see Experimental Section). Thus, polymerization of cyclic esters co-initiated by primary amines proceeds according to the following net equations:

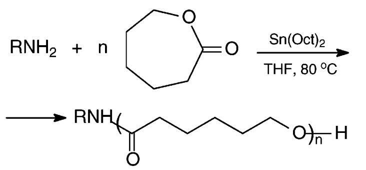

(2a)

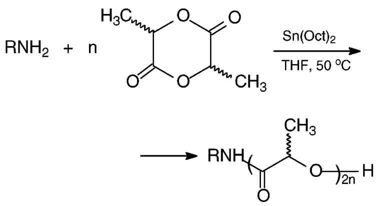

(2b)

A similar polymerization pathway has already been proposed for the high-temperature (≥160 °C) noncatalyzed primary-amine-initiated polymerization of the six- and seven-membered lactones.[21]

After determining structures of the polyester chains formed in the CL or LA/$Sn(Oct)_2$/$BuNH_2$ system, we studied kinetics of this polymerization. In all kinetic experiments, starting concentrations of monomers and that of tin(II) octoate initiator were kept constant: $[CL]_0 = 2$ mol L^{-1}, $[LA]_0 = 1$ mol L^{-1}, and $[Sn(Oct)_2]_0 = 0.05$ mol L^{-1}, whereas the starting concentration of $BuNH_2$ was changed in the range from 0 to 0.4 mol L^{-1}, i.e., $[BuNH_2]_0/[Sn(Oct)_2]_0 = 0 \div 8$. Polymerizations were conducted in THF as solvent at 80 °C (CL) or 50 °C (LA).

Results of the kinetic measurements are presented in the form of semilogarithmic coordinates in Figures 2 and 3. In the plots obtained for CL monomer (Figure 2), three kinetically distinguishable polymerization steps are clearly seen. The first one corresponds to the maximum relative rate ($r_p = -d[CL]/[CL]dt = \{\ln([CL]_0/[CL])\}/\Delta t$) of the CL monomer consumption. Concentration of monomer reacted in this step is approximately proportional to the starting concentration of $BuNH_2$ ($[BuNH_2]_0$). On the basis of the latter observation, we assumed that the polymerization starts from a direct reaction between CL and $BuNH_2$ catalyzed by $Sn(Oct)_2$ (eq 3).

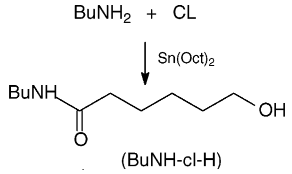

(3)

The separate kinetic measurements in the CL/$BuNH_2$ system (THF, 80 °C) revealed that the noncatalyzed [i.e., in the absence of $Sn(Oct)_2$] aminolysis of the CL monomer proceeds approximately 200 times slower than the catalyzed ones ($[Sn(Oct)_2] = 0.05$ mol L^{-1}) under the otherwise identical conditions.

Most probably, reaction of $BuNH_2$ with CL is preceded by the carboxylate−imide groups exchange at the tin atom in $Sn(Oct)_2$, accompanied by the octanoic acid (OctH) release (eq 4a). Afterward, it proceeds via CL monomer insertion between ...-Sn−NHBu bond with formation of the ...-Sn−O-$(CH_2)_5C(O)$-NHBu species (eq 4b). Finally, exchange reaction with OctH results in $BuNH[C(O)(CH_2)_5OH$ (eq 4c).

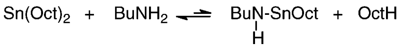

$$Sn(Oct)_2 + BuNH_2 \rightleftharpoons \underset{\textstyle H}{BuN}\text{-}SnOct + OctH \tag{4a}$$

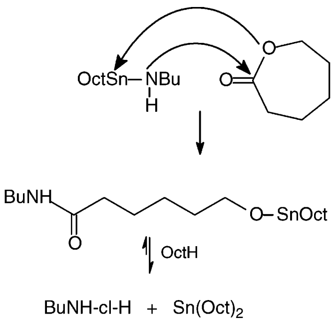

(4b)

(4c)

Thus, after the first step is completed, the initial mixture $Sn(Oct)_2$/$BuNH_2$ is converted into the $Sn(Oct)_2$/BuNH-m-H mixture (where m is the linear unimeric unit derived from CL or LA monomer) and, in principle, is equivalent to the $Sn(Oct)_2$/ROH (where ROH =

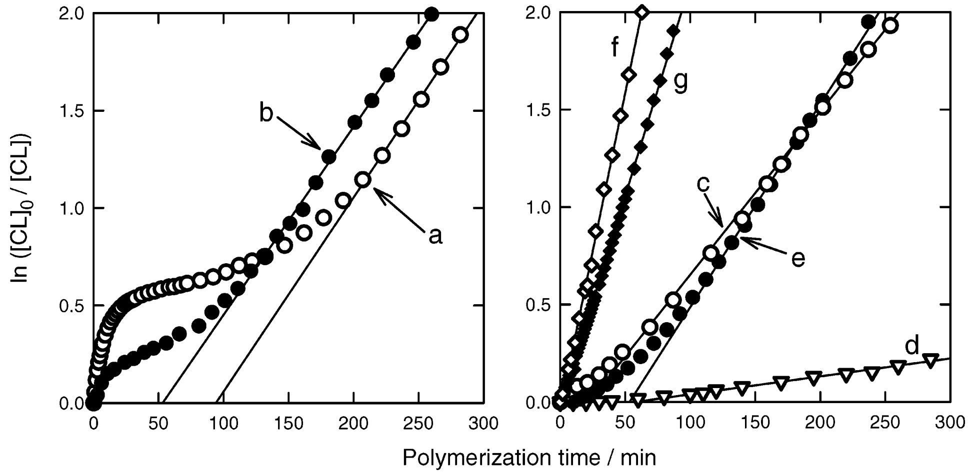

Figure 2. First-order kinetic dependencies for ϵ-caprolactone (CL) polymerization initiated with: $Sn(Oct)_2$/primary amine (a–e), tin(II) octoate [(tin(II) bis(2-ethylhexanoate), $(Sn(Oct)_2)$]/butyl alcohol (BuOH) (f), and $Sn(Oct)_2$/BuOH/*N*-methylacetamide (NMA) (g) mixtures. Conditions: $[CL]_0 = 2$ mol L^{-1}, $[Sn(Oct)_2]_0 = 0.05$ mol L^{-1}, $[NH_2]_0$ (in mol L^{-1}) = 0.40 (a), 0.18 (b), 0.05 (c, e), 0 (d); $[BuOH]_0 = 0.25$ mol L^{-1}, $[NMA]_0 = 0.25$ mol L^{-1}; amine: $C_4H_9NH_2$ (a–d), polyamino dendrimer bearing 32 NH_2 end groups (DAB–Am-32) (e); terahydrofuran (THF) solvent, 80 °C.

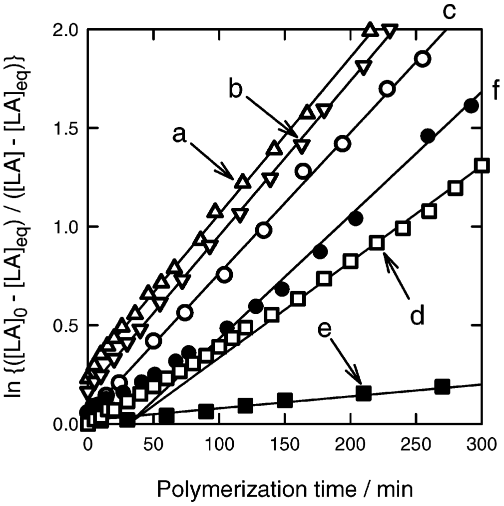

Figure 3. First-order kinetic dependencies for L,L-lactide (LA) polymerization initiated with tin(II) octoate [(tin(II) bis(2-ethylhexanoate), $(Sn(Oct)_2)$]/primary amine mixture. Conditions: $[LA]_0 = 1$ mol L^{-1}, $[Sn(Oct)_2]_0 = 0.05$ mol L^{-1}, $[NH_2]_0$ (in mol L^{-1}) = 0.26 (a), 0.14 (b), 0.05 (c, f), 0.016 (d), 0 (e); ($[LA]_{eq} = 0.055$ mol L^{-1});[26] amine: $C_4H_9NH_2$ (a–e), polyamino dendrimer bearing 32 NH_2 end groups (DAB–Am-32) (f); terahydrofuran (THF) solvent, 80 °C.

$BuNHC(O)(CH_2)_5OH$) system, already studied by us,[8–13] in which the carboxylate–alkoxide ligands exchange reaction takes place (eq 5a).

$$ROH + Sn(Oct)_2 \rightleftharpoons RO\text{-}SnOct + OctH \quad (5a)$$

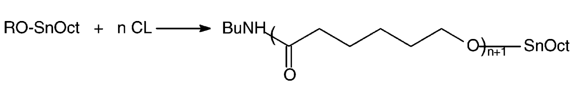

$$RO\text{-}SnOct + n\,CL \longrightarrow BuNH\!\left[C(O)(CH_2)_5O\right]_{n+1}\!\text{-}SnOct \quad (5b)$$

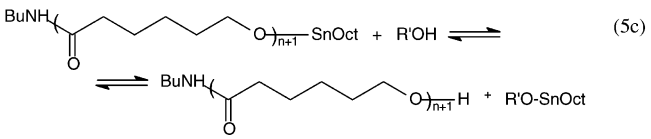

$$BuNH\!\left[C(O)(CH_2)_5O\right]_{n+1}\!\text{-}SnOct + R'OH \rightleftharpoons BuNH\!\left[C(O)(CH_2)_5O\right]_{n+1}\!H + R'O\text{-}SnOct \quad (5c)$$

The resulting tin(II)-alkoxide species initiates polymerization, and then propagation proceeds (eq 5b). Finally, the chain-transfer reaction provides the BuNH-$[C(O)(CH_2)_5O]_n$-H chains (eq 5c).

However, after the relatively fast initial period, the polymerization slows down, and the higher $[BuNH_2]_0$ is, the observed retardation effect is more pronounced (Figure 2, plots a and b). We tentatively ascribe this kinetic effect to a formation of the cyclic, intramolecular amide nitrogen-alkoxide/tin complex, resulting in the dormant species, as depicted in eq 6. It is known that tin(II) eagerly assumes tricoordinate pyramidal structure employing its empty p- or d-orbitals.[22,23]

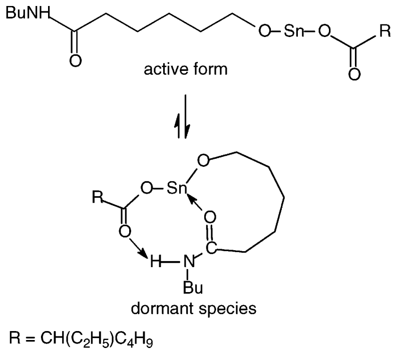

(6)

Presumably, the tin(II)–alkoxide bond in the intramolecularly coordinated species is more hindered and less polarized compared with the linear, noncoordinated ones, and thus is much less susceptible toward coordination with the forthcoming monomer. The doubly coordinated structure of the dormant species, shown in eq 6, is proposed by us on the basis of the DFT molecular orbital calculations using the Gaussian 03 program and carried out for the model $CH_3NHC(O)(CH_2)_5OSnO(O)CCH_3$ compound. The calculated difference in enthalpy between the intramolecularly bound conformation and the most stable open-chain one, $\Delta H = -69.5$ kJ mol^{-1}, also takes into account the ring-strain term. This kind of coordination is also possible via intermolecular reaction. Because $[Sn(Oct)_2]_0$ is relatively low, and additionally, equilibrium 4a is shifted into the left-hand side, the probability of this bimolecular coordination is substantially lower than that of the unimolecular one enhanced by the anchimeric assistance effect.

For oligomeric and then polymeric α-amido-ω-hydroxyl ($BuNH[C(O)(CH_2)_5O]_n$-SnOct) chains, the active–dormant species equilibrium becomes more shifted into

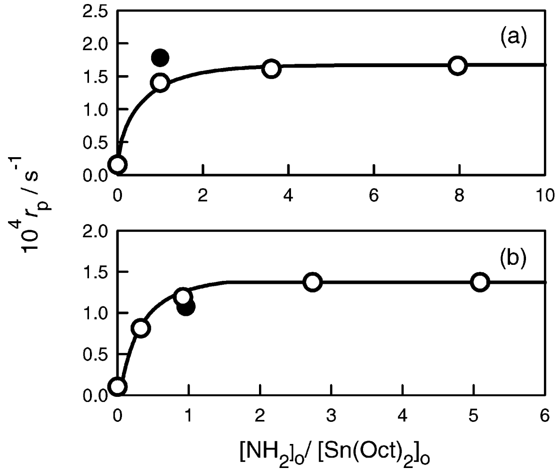

Figure 4. Dependence of the relative rate ($r_p = -d[\text{monomer}]/[\text{monomer}]dt = \{\ln([\text{monomer}]_0/[\text{monomer}])\}/\Delta t$) of the monomer consumption in cyclic ester polymerization initiated with tin(II) octoate [(tin(II) bis(2-ethylhexanoate), ($Sn(Oct)_2$)]/primary amine system on the $[NH_2]_0/[Sn(Oct)_2]_0$ ratio. Monomer: ϵ-caprolactone [CL, (a)] and L,L-lactide [LA, (b)]. Conditions: $[Sn(Oct)_2]_0 = 0.05$ mol L^{-1}, $[CL]_0 = 2$ mol L^{-1}, 80 °C; $[LA]_0 = 1$ mol L^{-1}, 50 °C; amine: $C_4H_9NH_2$ (hollow circles), polyamino dendrimer bearing 32 NH_2 end groups (DAB−Am-32) (filled circles); terahydrofuran (THF) solvent.

the linear active species side with an increase in their polymerization degree, in agreement with the Jacobson−Stockmayer theory.[24,25] Therefore, the polymerization accelerates with monomer consumption, and eventually, r_p becomes constant. In principle, we should expect the final r_p's identical with those obtained for the CL/$Sn(Oct)_2$/BuOH system[8] under the otherwise comparable conditions. Actually, r_p's determined in the present paper are considerably lower than expected. This result suggests that the intermolecular coordination cannot be completely neglected. Indeed, comparison of polymerization kinetics in CL/$Sn(Oct)_2$/BuOH and CL/$Sn(Oct)_2$/BuOH/*N*-methylacetamide (NMA) systems (Figure 2, plots f and g) points to the remarkable retardation effect caused by NMA.

Kinetic plots obtained for the LA/$Sn(Oct)_2$/$BuNH_2$ system (Figure 3) also reveal rapid initial LA monomer consumption with the rate proportional to $[BuNH_2]_0$, however, no retardation is observed. Most probably, the secondary alkoxide structure and the rigid alkylene chain in the unimeric $BuNHC(O)CH(CH_3)OC(O)CH(CH_3)O-SnOct$ species prohibit the intramolecular coordination, in contrast to the $BuNHC(O)(CH_2)]_5O-SnOct$ species (eq 6). However, intermolecular coordination cannot be excluded because, in comparison with LA/$Sn(Oct)_2$/BuOH system,[11] r_p's determined in the present paper are lower, as in the CL polymerization case discussed above.

In Figure 4, results of the kinetic measurements are presented in coordinates relating polymerization rates (r_p) and $[BuNH_2]_0/[Sn(Oct)_2]_0$ ratios (r_p's are equivalent to the slopes of the linear regressions plotted for the kinetic runs in Figures 2 and 3). Initially, polymerization rate increases with increasing $[BuNH_2]_0/[Sn(Oct)_2]_0$ ratio, and for the higher $[BuNH_2]_0/[Sn(Oct)_2]_0$ values, it levels off. This type of kinetic behavior has been already reported by us for the cyclic ester/$Sn(Oct)_2$/ROH system[8,11] and corresponds to the mechanism in which the carboxylate−alkoxide exchange (eq 1) is followed by the polyester chain growth on the tin(II) alkoxide species.

Synthesis of the Star-Shaped Polyesters on the Polypropyleneimine Dendrimer Core. Various practically important properties of poly(aliphatic ester)s such as solution or melt viscosity, degradation rate, or mechanical and thermal parameters can be adjusted by the macromolecular architecture (topology). Particularly interesting properties are provided by the branched or star-shaped polymers, which can be prepared with multifunctional initiators/chain-transfer agents. In the cyclic esters polymerization, polyols were most often employed for this purpose (see, e.g., refs 27−32). For example, in our recent paper, we describe application of various polyols $[R-(OH)_x]$ containing exclusively primary hydroxyl groups: diethyleneglycol ($x = 2$), trimethylolpropane ($x = 3$), di(trimethylolpropane) ($x = 4$), dipentaerithritol ($x = 6$), and poly(3-ethyl-3-hydroxymethyl-oxetane) ($\langle x \rangle = 13$) as co-initiators/transfer agents for synthesis polymerization of the corresponding star-shaped PLA's.[32]

However, availability of the soluble polyols enabling, e.g., molar masses control of the star-shaped polyesters, is rather limited. This was one of the reasons that we decided to check a possibility of using for a similar purpose another class of multifunctional reagents, polyamines, able to co-initiate (in the presence of $Sn(Oct)_2$) polymerization of cyclic esters. These derivatives have been applied for synthesis of the star-shaped polymers only recently, namely by means of grafting of living poly(tetrahydrofuran) onto amino dendrimers of various generations.[33]

We report the preliminary results on preparation of star-shaped PCL and PLA starting from dendrimers fitted with 8 and 32 terminal amino groups (see structures DAB−Am-8 and DAB−Am-32 shown below). Kinetic data reported in the preceding section show that the DAB−Am-32 polyamine dendrimer is able to co-initiate CL and LA polymerization, giving r_p's similar to those determined for $BuNH_2$ (Figure 4, filled points). This result strongly suggests that all NH_2 groups in DAB−Am-32 take part in the polymer chain growth, eventually giving the regular, star-shaped polyester. The latter conclusion is supported by the molar-mass characteristics for the polyesters, prepared on the DAB−Am-8 and DAB−Am-32 cores, collected in Table 1.

DAB-Am-8

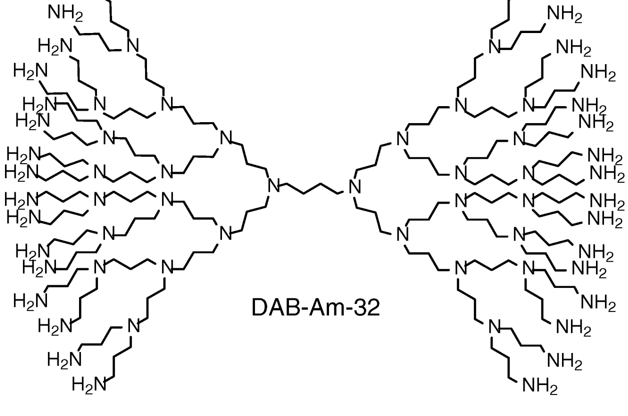

DAB-Am-32

Table 1. Comparison of M_n's of the Star-Shaped Poly(ε-caprolactones) (PCL) and Poly(L-lactide)s (PLA) Determined by SEC-MALLS, Osmometry, and ^1H NMR[a]

dendrimer monomer	$([M]_0 - [M]_{eq})/[DAB]_0$	M_n[b] (calcd)	M_n (osm.)	M_n (NMR)	M_n[e] (SEC)	M_w/M_n[e] (SEC)
DAB−Am-8 (L,L)-LA	47.4	7600	6400[c]	7000		
DAB−Am-8 CL	58.9	7500	6900[c]	7500		
DAB−Am-8 (L,L)-LA	688.5	100000	87200[d]		103700	1.03
DAB−Am-8 CL	858	98700	79600[d]	79000	114000	1.04
DAB−Am-32 (L,L)-LA	2075	302600	253600[d]	285000	376900	1.02
DAB−Am-32 CL	2607	301100	230200[d]	287500	373000	1.05
DAB−Am-32 (D,D)-LA	2051	299100	208100[d]	291000	356400	1.03

[a] $[LA]_0 = 1.5$ mol L^{-1}, $[CL]_0 = 2.0$ mol L^{-1}, $[Sn(Oct)_2]_0 = 2 \times 10^{-3}$ mol L^{-1}, THF solvent, 80 °C. [b] Calculated according to eq 7. [c] Vapor-pressure osmometry. [d] High-speed membrane osmometry. [e] Laser light scattering detector.

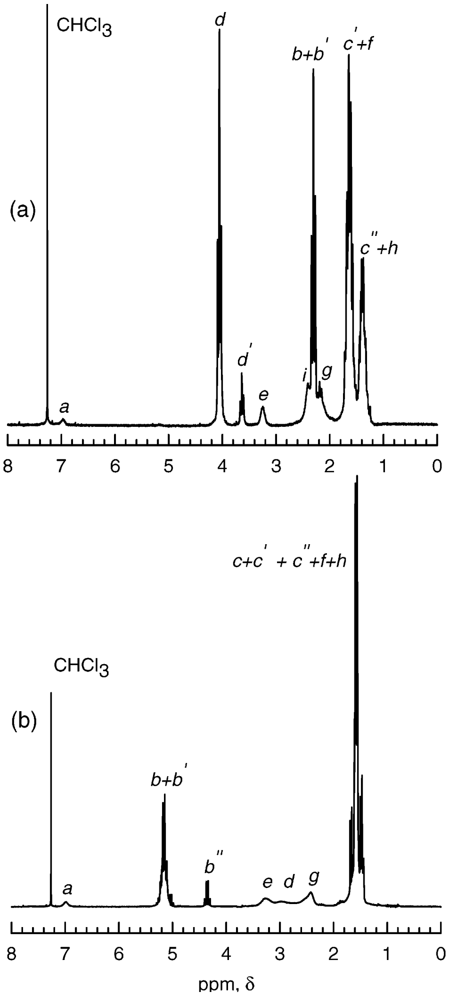

Figure 5. ^1H NMR spectra of the star-shaped poly(ε-caprolactone (PCL), $[CL]_0/[DAB]_0 = 2607$ (a) and poly(L-lactide) (PLA), $([LA]_0 - [LA]_{eq})/[DAB]_0 = 2075$ (b) prepared with Sn(Oct)$_2$/polyamino DAB−Am-32 dendrimer.

Although there is a certain scatter of the experimental M_n's determined from SEC, osmometric, and ^1H NMR measurements, these values are in a good agreement, within the expected experimental error, with the theoretically predicted molar masses (M_n(calcd)). Moreover, molar-mass distributions are narrow (cf. M_w/M_n column).

The net reaction scheme for synthesis of the star-shaped polyester based on the polyamino dendrimer reads:

$$R(NH_2)_x + nx\,M \rightarrow R[NH\text{-}(m)_n\text{-}H]_x \qquad (7)$$

Assuming that chain-transfer side reactions are excluded, the expected molar masses M_n(calcd) can be calculated from the simple expressions, usually applicable for a living polymerization mechanism:

$$M_n(\text{calcd}) = M_M\,([M]_0 - [M]_{eq})/[DAB]_0 + M_{DAB} \qquad (8)$$

where M_M denotes molar mass of CL or LA (114.14 or 144.13, respectively); M_{DAB} the molar mass of DAB−Am-8 or DAB−Am-32 (773.3 or 3514, respectively)].

Figure 5 shows examples of ^1H NMR spectra of the PCL and PLA star-shaped polymers prepared with DAB−Am-32 as co-initiator. Signals marked in the spectra can be ascribed to the corresponding protons as shown in the structures below.

For PCL:

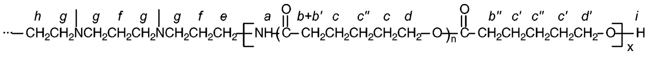

$$\cdots CH_2CH_2NCH_2CH_2CH_2NCH_2CH_2CH_2-[NH(\overset{O}{\overset{\|}{C}}-CH_2CH_2CH_2CH_2CH_2-O)_n\overset{O}{\overset{\|}{C}}-CH_2CH_2CH_2CH_2CH_2-O]_x-H$$

and for PLA:

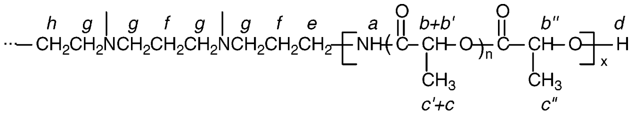

$$\cdots CH_2CH_2NCH_2CH_2CH_2NCH_2CH_2CH_2-[NH(\overset{O}{\overset{\|}{C}}-\underset{CH_3}{\underset{|}{CH}}-O)_n\overset{O}{\overset{\|}{C}}-\underset{CH_3}{\underset{|}{CH}}-O]_x-H$$

Because all primary amino groups in dendrimers started polyester chain growth, as suggested by results of the kinetic measurements, it is possible to employ the pertinent ^1H NMR spectra to calculate molar masses of the resulting star-shaped polyesters. In the case of PCL:

$$M_n = xM_{CL}[I(d) + I(d')]/I(d') + M_{DAB} \qquad (10)$$

(where I's denote integrations of the corresponding signals, and M's the corresponding molar masses; $x = 8$ or 32). Similarly for PLA:

$$M_n = xM_{LA}[I(b) + I(b') + I(b'')]/I(b'') + M_{DAB} \qquad (11)$$

Conclusions

The present work shows that mechanism of polymerization in the ε-caprolactone or L,L-lactide/tin octoate [Sn(Oct)$_2$]/primary amine (RNH_2) system does not differ appreciably from that co-initiated with alcohol (ROH). In the first step of polymerization initiated with the Sn(Oct)$_2$/RNH_2 mixtures, formation of the α-amido-ω-alcohol [RNH-m-H (R′OH)] takes place. Then, eventually, the Sn(Oct)$_2$/RNH_2-initiated polymerization proceeds by a monomer insertion into the ...-Sn−OR″ bond, reversibly formed in the reaction ...-SnOct + R″OH $\rightleftharpoons$ ...-Sn−OR″ + OctH, where R″OH is either the low-molar-mass co-initiator (R′OH) or a macromolecule fitted with hydroxyl end group [RNH-(m)$_n$-H)].

Successful and controlled polymerization in the presence of simple primary amine or polyamino dendrimers provides further arguments that the mechanism assuming formation of the secondary oxonium ions (including activated monomer mechanism) or initiation with carboxylic acid does not operate.

Acknowledgment. This work was supported by the Polish State Committee for Scientific Research (KBN), grant numbers: 3 T09A 002 27 and PBZ-KBN-070/T09/2001/2 for the period: 2003-2006.

References and Notes

(1) Leenslag, J. W.; Pennings, A. J. *Makromol. Chem.* **1987**, *188,* 1809−1814.

(2) Nijenhuis, A. J.; Grijpma, D. W.; Pennings, A. J. *Macromolecules* **1992**, *25*, 6419−6424.

(3) Doi, Y. J.; Lemstra, P. J.; Nijenhuis, A. J.; van Aert, H. A. M.; Bastiaansen, C. *Macromolecules* **1995**, *28*, 2124−2132.

(4) Schwach, G.; Coudane, J.; Engel, R.; Vert, M. *J. Polym. Sci., Part A: Polym. Chem.* **1997**, *35*, 3431−3440.

(5) Kricheldorf, H. R.; Kreiser-Saunders: I.; Boettcher, C. *Polymer* **1995**, *36*, 1253−1259.

(6) Zhang, X.; MacDonald, D. A.; Goosen, M. F. A.; McAuley, K. B. *J. Polym. Sci., Part A: Polym. Chem.* **1994**, *32*, 2965−2970.

(7) In't Veld, P. J. A.; Velner, E. M.; van de Witte, P.; Hamhuis, J.; Dijkstra, P. J.; Feijen, J. *J. Polym. Sci., Part A: Polym. Chem.* **1997**, *35*, 219−226.

(8) Kowalski, A.; Duda, A.; Penczek, S. *Macromol. Rapid Commun.* **1998**, *19*, 567−572.

(9) Kowalski, A.; Duda, A.; Penczek, S. *Macromolecules* **2000**, *33*, 689

(10) Kowalski, A.; Libiszowski, J.; Duda, A.; Penczek, S. *Macromolecules* **2000**, *33*, 1964−1971.

(11) Kowalski, A.; Duda, A.; Penczek, S. *Macromolecules* **2000**, *33*, 7359−7370.

(12) Majerska, K.; Duda, A.; Penczek, S. *Macromol. Rapid Commun.* **2000**, *21*, 1327−1332.

(13) Duda, A.; Penczek, S.; Kowalski, A.; Libiszowski, J. *Macromol. Symp.* **2000**, *153*, 41−53.

(14) Cai, Q.; Zhao, Y.; Bei, J.; Xi, F.; Wang, S. *Biomacromolecules* **2003**, *4*, 828−834.

(15) Liu, J.; Liu, L. *Macromolecules* **2004**, *37*, 2674.

(16) Dubois, P.; Degee, P.; Jerome, R.; Teyssie, P. *Macromolecules* **1992**, *25*, 2614−2618.

(17) Frisch, M. J.; Trucks, G. W.; Schlegel, H. B.; Scuseria, G. E.; Robb, M. A.; Cheeseman, J. R.; Montgomery, J. A., Jr.; Vreven, T.; Kudin, K. N.; Burant, J. C.; Millam, J. M.; Iyengar, S. S.; Tomasi, J.; Barone, V.; Mennucci, B.; Cossi, M.; Scalmani, G.; Rega, N.; Petersson, G. A.; Nakatsuji, H.; Hada, M.; Ehara, M.; Toyota, K.; Fukuda, R.; Hasegawa, J.; Ishida, M.; Nakajima, T.; Honda, Y.; Kitao, O.; Nakai, H.; Klene, M.; Li, X.; Knox, J. E.; Hratchian, H. P.; Cross, J. B.; Bakken, V.; Adamo, C.; Jaramillo, J.; Gomperts, R.; Stratmann, R. E.; Yazyev, O.; Austin, A. J.; Cammi, R.; Pomelli, C.; Ochterski, J. W.; Ayala, P. Y.; Morokuma, K.; Voth, G. A.; Salvador, P.; Dannenberg, J. J.; Zakrzewski, V. G.; Dapprich, S.; Daniels, A. D.; Strain, M. C.; Farkas, O.; Malick, D. K.; Rabuck, A. D.; Raghavachari, K.; Foresman, J. B.; Ortiz, J. V.; Cui, Q.; Baboul, A. G.; Clifford, S.; Cioslowski, J.; Stefanov, B. B.; Liu, G.; Liashenko, A.; Piskorz, P.; Komaromi, I.; Martin, R. L.; Fox, D. J.; Keith, T.; Al-Laham, M. A.; Peng, C. Y.; Nanayakkara, A.; Challacombe, M.; Gill, P. M. W.; Johnson, B.; Chen, W.; Wong, M. W.; Gonzalez, C.; Pople, J. A. *Gaussian 03*, revision C.02; Gaussian, Inc.: Wallingford, CT, 2004.

(18) Becke, A. D. *J. Chem. Phys.* **1993**, *98*, 5648−5652.

(19) Dunning, T. H., Jr.; Hay, P. J. In *Modern Theoretical Chemistry*; Schaefer, H. F., III., Ed.; Plenum Press: New York, 1976; Vol. 3, p 1.

(20) Hay, P. J.; Wadt, W. R. *J. Chem. Phys.* **1985**, *82*, 299−310.

(21) Saotome K., Kodaira Y. *Makromol. Chem.* **1965**, *82*, 41−52.

(22) Donaldson, J. D.; Jelen, A. *J. Chem. Soc. A* **1968**, 1448−1450.

(23) Birchal, T. Faggiani, R.; Lock, C. J. L.; Manivannan, V. *J. Chem. Soc., Dalton. Trans.* **1987**, 1675−1682.

(24) Jacobson, H.; Stockmayer, W. H. *J. Chem. Phys.* **1950**, *18*, 1600−1606.

(25) Semlyen, J. A. *Adv. Polym. Sci.* **1976**, *21*, 43−75.

(26) Duda, A.; Penczek, S. *Macromolecules* **1990**, *23*, 1636−1639.

(27) Spinu, M.; Jackson, C.; Keating, M. Y.; Gardner, K. H. *J. Macromol. Sci., Pure Appl. Chem.* **1996**, *A33*, 1497−1530.

(28) Lee, S.-H.; Kim, S. H.; Han, Y. K.; Kim, Y. H. *J. Polym. Sci., Part A: Polym. Chem.* **2001**, *39*, 973−985.

(29) Zhao, Y. L.; Cai, Q.; Jiang, J.; Shuai, X. T.; Bei, J. Z.; Chen, C. F.; Xi, F. *Polymer* **2002**, *43*, 5819−5825.

(30) Sanda, F.; Sanada, H.; Shibasaki, Y.; Endo, T. *Macromolecules* **2002**, *35*, 680−683.

(31) Ydens, Y.; Degee, Ph.; Dubois, Ph.; Libiszowski, J.; Duda, A.; Penczek, S. *Macromol. Chem. Phys.* **2003**, *204*, 171−179.

(32) Biela, T.; Duda, A.; Rode, K.; Pasch, H. *Polymer* **2003**, *44*, 1851−1860.

(33) Tanghe, L. M.; Goethals, E. J. *e-Polymers* **2001**, *017*, 1−11 (http://www.e-polymers.org/papers/goethals_070901.pdf).

MA050752J